Diagrammatic, self-consistent treatment of the Anderson localization problem in d ≤ 2 dimensions

Dieter Vollhardt, P. Wölfle

Diagrammatic, self-consistent treatment of the Anderson localization problem in $d \leq 2$ dimensions

D. Vollhardt and P. Wölfle

Max-Planck-Institut für Physik und Astrophysik, Munich, Federal Republic of Germany
and Physik Department, Technische Universität München, Garching, Federal Republic of Germany
(Received 21 July 1980)

A standard diagrammatic theory is formulated for the density response function $\chi(\vec{q},\omega)$ of a system of independent particles moving in a random potential. In the limit of small $\vec{q},\omega$ the Bethe-Salpeter equation for the particle-hole vertex function may be solved for $\chi(\vec{q},\omega)$ in terms of a current relaxation kernel $M(\vec{q},\omega)$ [essentially the inverse of the diffusion coefficient $D(\vec{q},\omega)$]. $M(\vec{q},\omega)$ is obtained as the sum of the imaginary part of the single-particle self-energy and the current matrix element of the irreducible kernel and is determined diagrammatically. A theorem is formulated, stating that *any* diagram for $M(0,\omega)$ or $D(0,\omega)$ containing a (bare) diffusion propagator belongs to a well-defined class of diagrams whose divergencies cancel each other, and an exact proof is presented. In particular, this implies that there are no divergent contributions to $M(0,\omega)$ or $D(0,\omega)$ from a diffusion propagator. However, in the presence of time-reversal invariance, $M(\vec{q},\omega)$ is shown to have infrared divergencies in $d \leq 2$, signalling a breakdown of the perturbation expansion in terms of the scattering potential which has first been discussed by Abrahams *et al*. A self-consistent treatment in the weak-coupling limit yields a finite static polarizability α, a dynamical conductivity $\text{Re}\sigma(\omega) \propto \omega^2$ for $\omega \rightarrow 0$, and a finite localization length in $d \leq 2$ for arbitrarily weak disorder. In $d = 1$ our results agree remarkably well with the exact solutions by Berezinsky and also Abrikosov and Ryshkin. Ryshkin.

I. INTRODUCTION

Initiated by the pioneering paper of Anderson,[1] the problem of localization of a quantum-mechanical particle subject to a random potential has attracted great attention ever since. It is well known that in dimension $d = 3$ particles moving in a random potential (e.g., generated by impurities) will, in general, not be able to move in the system, i.e., will be localized if either the potential fluctuations exceed a certain threshold value[1] or if (at given disorder) the particle energy is low enough.[2] In these cases such a system undergoes an Anderson transition. On the other hand, for a one-dimensional system the general consensus[3] has long since been that it will always be localized irrespective of how small the disorder may be.

Recently, the field has gained new impetus by two developments: the application of renormalization-group ideas[4-7] and the formulation of a self-consistent mode-coupling theory for the Anderson transition.[8] In particular, Abrahams *et al.*[5] proposed a one-parameter scaling theory for the conductance of a finite sample as a function of L, the sample dimension. By determining the scaling function in the two limits of small and large conductance by perturbation theory they were able to show that the particles in a random potential are always localized for $d \lesssim 2$ dimensions irrespective of the strength of disorder. The result for $d = 2$ has been questioned by Lee,[7] who

claims to have evidence for an Anderson transition in $d = 2$ from numerical studies of the real-space renormalization transformation. On the other hand, Götze[8] has calculated the detailed behavior of the density response function in the localized and the extended regimes including the Anderson transition for $d = 3$. His results are consistent with exact scaling laws in the vicinity of the Anderson transition but cover a much broader range of parameters.

In this context it has been our intention to approach the problem of Anderson localization by means of a standard diagrammatic theory. Rather than studying the one-particle properties of the system under consideration, our aim has been to derive a two-particle formalism which allows us to calculate response functions of such a system (e.g., the density response function) in terms of a current relaxation kernel $M(\vec{q}, \omega)$. We believe that in doing so, the present paper presents a unification of the concepts of a mode-coupling theory with those of a standard diagrammatic analysis. Such a framework allows us to obtain quantitative results for the transport properties of disordered systems, e.g., for the dynamical conductivity or the static polarizability. Our theory is based on an extended state formalism within an Edwards model,[9] which is particularly suited for a diagrammatic treatment. The present analysis deals with the weak-coupling regime, where perturbation theory in the disorder parameter is a useful starting point. In order to obtain local-

4666

ization in this limit the perturbation expansion must contain divergent terms. We systematically investigate the possibilities to have infrared divergent contributions to the current relaxation kernel, which are easily seen to exist only for $d \leqslant 2$. By renormalizing the density propagator in the leading divergent contributions we are led to a self-consistent equation which may easily be solved to yield explicit expressions for the density response functions at small $\vec{q}, \omega$.

The paper is structured as follows. In Sec. II, the basis for the density response theory is given; then, in Sec. III, the infrared divergent contributions to the current relaxation kernel $M(\vec{q}, \omega)$ are determined. Finally, in Secs. IV and V the results are presented and discussed.

II. DENSITY RESPONSE THEORY

Our analysis employs the model of independent electrons moving in a potential provided by randomly distributed static impurity scattering centers with density n_i at $T = 0$. The interaction of the electrons with the impurities is described by the following Hamiltonian:

$$H = \int d\vec{r}\, \psi^\dagger(\vec{r}) \left(-\frac{\nabla^2}{2m} + \sum_i V(\vec{r} - \vec{r}_i) \right) \psi(\vec{r}) . \quad (1)$$

Here $V(\vec{r} - \vec{r}_i)$ is the potential of an impurity at the random position $\vec{r}_i$ as felt by an electron at position $\vec{r}$ (the following analysis may also be generalized to other types of disorder). The formulation of the one-particle problem at $T = 0$ via Green's functions can easily be carried out by means of the standard methods of field theory.[10] Accordingly, we introduce the one-particle Green's function as

$$G(\vec{r}, \vec{r}') = -i\langle \phi_0 | T[\psi^\dagger(\vec{r})\psi(\vec{r}')] | \phi_0 \rangle , \quad (2)$$

where $|\phi_0\rangle$ is the ground state of the interacting system. The Fourier transform of $G(\vec{r}, \vec{r}')$ can be written as

$$G(\vec{p}, \vec{p}'; \omega) = \sum_n \varphi_n(\vec{p}) \varphi_n^*(\vec{p}') \left(\frac{1 - f_n}{\omega - \epsilon_n + i0} + \frac{f_n}{\omega - \epsilon_n - i0} \right) , \quad (3)$$

where $\varphi_n(\vec{p})$ are the eigenstates of H corresponding to the energy ϵ_n; the f_n $[= f(\epsilon_n)]$ are the usual Fermi functions. The retarded and advanced Green's functions are defined as

$$G^{R,A}(\vec{p}, \vec{p}'; \omega) = \sum_n \frac{\varphi_n(\vec{p}) \varphi_n^*(\vec{p}')}{\omega - \epsilon_n \pm i0} , \quad (4)$$

so that the Green's function for the noninteracting fermion system is given by

$$G^0(\vec{p}, \vec{p}'; \omega) = \frac{\delta(\vec{p} - \vec{p}')}{\omega - p^2/2m + i\delta \, \text{sgn}(|\vec{p}| - p_F)} . \quad (5)$$

We will now turn to the formulation of the two-particle problem. For this we introduce the density response function $\chi(\vec{r}, \vec{r}'; \omega)$:

$$\chi(\vec{r}, \vec{r}'; \omega) = i \int_0^\infty dt\, e^{i(\omega + i0)t} \langle \phi_0 |[\rho(\vec{r}, t), \rho(\vec{r}', 0)]_- | \phi_0 \rangle$$

$$= \sum_{n, n'} \varphi_n^*(\vec{r}) \varphi_{n'}(\vec{r}) \varphi_{n'}^*(\vec{r}') \varphi_n(\vec{r}') \frac{f_{n'} - f_n}{\omega - \epsilon_n - \epsilon_{n'}} , \quad (6)$$

where the density operator $\rho(\vec{r})$ is defined by

$$\rho(\vec{r}) = \psi^\dagger(\vec{r})\psi(\vec{r}) = \sum_{n, n'} \varphi_n^*(\vec{r}) \varphi_{n'}(\vec{r}) a_n^\dagger a_{n'} . \quad (7)$$

As the impurities are supposed to be distributed randomly in the system we can average over the impurity positions[10] and therefore obtain for the Fourier transform of $\langle \chi(\vec{r}, \vec{r}'; \omega) \rangle = \chi(\vec{r} - \vec{r}'; \omega)$

$$\chi(\vec{q}, \omega) = \sum_{\vec{p}, \vec{p}'} \sum_{n, n'} \left\langle \varphi_{n'}(\vec{p}_+) \varphi_{n'}^*(\vec{p}'_+) \varphi_n(\vec{p}'_-) \varphi_n^*(\vec{p}_-) \frac{f_{n'} - f_n}{\omega + \epsilon_n - \epsilon_{n'}} \right\rangle \quad (8a)$$

$$= \sum_{\vec{p}, \vec{p}'} \frac{1}{2\pi i} \int_{-\infty}^\infty dE \{ [f(E + \omega) - f(E)] \langle G^R(\vec{p}_+, \vec{p}'_+; E + \omega) G^A(\vec{p}'_-, \vec{p}_-; E) \rangle$$

$$+ f(E) \langle G^R(\vec{p}_+, \vec{p}'_+; E + \omega) G^R(\vec{p}'_-, \vec{p}_-; E) \rangle - f(E + \omega) \langle G^A(\vec{p}_+, \vec{p}'_+; E + \omega) G^A(\vec{p}'_-, \vec{p}_-; E) \rangle \} . \quad (8b)$$

In (8b) we have expressed (8a) by means of pairs of advanced and retarded single-particle Green's functions, $\langle \rangle$ implies impurity averaging and $\vec{p}_\pm = \vec{p} \pm \vec{q}/2$. Before we evaluate (8b) further let us discuss some of its analytic properties. For abbreviation let us write

$$\chi(\vec{q}, \omega) = - \int_{-\infty}^\infty dE \{ [f(E + \omega) - f(E)] \phi^{RA}(E, \omega; \vec{q}) + f(E) \phi^{RR}(E, \omega; \vec{q}) - f(E + \omega) \phi^{AA}(E, \omega; \vec{q}) \} , \quad (9)$$

where we have introduced

$$\phi^{RA}(E, \omega; \vec{q}) = -\frac{1}{2\pi i} \sum_{\vec{p}, \vec{p}'} \langle G^R(\vec{p}_+, \vec{p}'_+; E + \omega) G^A(\vec{p}'_-, \vec{p}_-; E) \rangle , \quad (10)$$

etc. For small $\vec{q}$ and ω we can readily see that ϕ^{RR} and ϕ^{AA} are finite and nonzero. In the limit $q \to 0, \omega \to 0$ one has $G^A(\vec{p}, \vec{p}'; E) = [G^R(\vec{p}', \vec{p}; E)]^*$ and therefore $\phi^{RR}(E, 0; 0) = -[\phi^{AA}(E, 0; 0)]^*$. Using

$$\phi^{RR}(E,0;0) = \frac{1}{2\pi i} \sum_{\vec{p},\vec{p}'} \partial \langle G^R \rangle / \partial E$$

and

$$\int dE f(E) \, \text{Im}[-2\pi i \, \phi^{RR}(E,0;0)] = \pi N(E_F) \, ,$$

where $N(E_F)$ is the density of states at the Fermi energy E_F, and furthermore $f(E+\omega) - f(E) = -\omega\delta(E)$ for $\omega \to 0$ and $T=0$, Eq. (9) can be written as[10]

$$\chi(\vec{q},\omega) = \omega\phi(\vec{q},\omega) + \chi^T + O(\omega,q^2) \, . \qquad (11)$$

Here we have introduced

$$\phi(\vec{q},\omega) = \sum_{\vec{p},\vec{p}'} \phi_{\vec{p}\vec{p}'} \equiv \phi^{RA}(E_F,\omega;\vec{q}) \, ,$$

and $\chi^T = N(E_F)$ is the isothermal compressibility. For $q=0$ (limit of infinite wavelength) the density response function $\chi(\vec{q},\omega)$ vanishes (particle conservation) and therefore we have[11]

$$\phi(0,\omega) = -\frac{N(E_F)}{\omega} \, , \qquad (12)$$

i.e., $\phi(0,\omega) [\equiv \phi^{RA}(0,\omega)]$ diverges for $\omega \to 0$. It is interesting to note that the function $\phi = (\chi - \chi^T)/\omega$ is identical to the relaxation function as introduced in mode-coupling theories.[8]

In the next step we want to introduce the interaction between the electrons and the random impurities. For this a perturbation theory for $\langle G^R G^A \rangle$ has to be formulated. We will here employ a renormalized perturbation theory by means of skeleton diagrams, i.e., diagrams for the self-energy and the vertex function without any self-energy insertions. Typical diagrams contributing to $\langle G^R G^A \rangle$ are shown in Fig. 1, where dashed lines correspond to electron-impurity interactions, every line being associated with a factor

$$U_0(\vec{p}-\vec{p}') = n_i \left| V(\vec{p}-\vec{p}') \right|^2 \, ,$$

where n_i is the density of the impurities and $V(\vec{p})$

FIG. 1. Typical diagrams of the perturbation theory for the impurity average $\langle G^R_{\vec{p}_+} G^A_{\vec{p}_-} \rangle$ are shown.

is the Fourier transform of the scattering potential. Furthermore, a solid line represents the averaged single-particle Green's functions $G^{R,A}_{\vec{p}}$ given by

$$G^R_{\vec{p}} = [E_F + \omega - p^2/2m - \Sigma^R_{\vec{p}}(E_F + \omega)]^{-1} \, ,$$

$$G^A_{\vec{p}} = [E_F - p^2/2m - \Sigma^A_{\vec{p}}(E_F)]^{-1} \, , \qquad (13)$$

where $\Sigma^{R,A}_{\vec{p}}$ is the self-energy. To lowest order in n_i and $V(\vec{q})$ one obtains (Born approximation)

$$\gamma \equiv \text{Im}\Sigma^A_{p_F}(E_F) \simeq \pi N(E_F) \int \frac{d\Omega_{\vec{p}'}}{4\pi} U_0(\vec{p}_F - \vec{p}_F') \, . \qquad (14)$$

Assuming the scattering centers to be pointlike, we have $U_0(\vec{p}-\vec{p}') = U_0$. As the impurity concentration n_i is supposed to be small (weak-coupling limit) γ is much smaller than the particle energy ($\gamma/E \ll 1$). In this case single-particle quantities are smoothly varying functions of disorder and one expects only small changes, e.g., in the density of states. This is the reason why the low-order perturbation expressions for G^R and G^A as given by (13) and (14) are sufficient for our purpose of calculating the singular behavior in ω of two-particle properties like the density correlation function.

All the diagrams in Fig. 1 can be classified into reducible and irreducible ones, depending on whether or not a diagram can be broken into two separate parts by simply cutting an electron and a hole line. It is convenient to introduce a vertex function $\Gamma_{\vec{p}\vec{p}'}(\vec{q},\omega)$ defined by

$$\phi_{\vec{p}\vec{p}'}(\vec{q},\omega) = -\frac{1}{2\pi i} G^R_{\vec{p}_+} G^A_{\vec{p}_-} [\delta_{\vec{p}\vec{p}'} + \Gamma_{\vec{p}\vec{p}'}(\vec{q},\omega) G^R_{\vec{p}'_+} G^A_{\vec{p}'_-}] \, , \qquad (15)$$

which contains irreducible as well as reducible diagrams as shown in Fig. 2. One subclass of (reducible) diagrams to $\Gamma_{\vec{p}\vec{p}'}$ are pure ladder diagrams which can be summed up immediately to yield the partial sum $\Gamma^0_{\vec{p}\vec{p}'}(\vec{q},\omega)$ (see Fig. 3) where

$$\Gamma^0_{\vec{p}\vec{p}'}(\vec{q},\omega) = \frac{U_0}{1 - U_0 \sum_{\vec{p}} G^R_{\vec{p}_+} G^A_{\vec{p}_-}}$$

$$= \frac{U_0 \gamma}{-i\omega + D_0 q^2} \, . \qquad (16)$$

Hence Γ^0 has a diffusion pole for $q \to 0$, $\omega \to 0$ which is due to the cancellation of the $\omega, \vec{q}$ independent term in the denominator of Γ^0 (a consequence of particle conservation). Therefore Γ^0 is called the (bare) diffusion propagator. The diffusion constant D_0 is given by $D_0 = E_F/(md\gamma)$, where d is the dimension of the system.

It is very instructive to observe that in the case of time-reversal invariance the full vertex func-
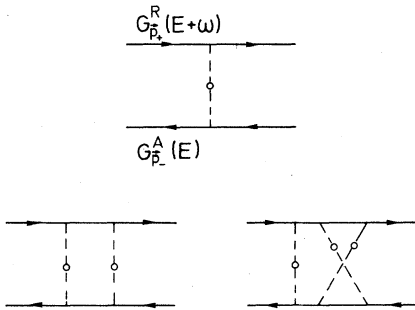
$$\Gamma_{\vec{p}\vec{p}'}(\vec{q},\omega) =$$

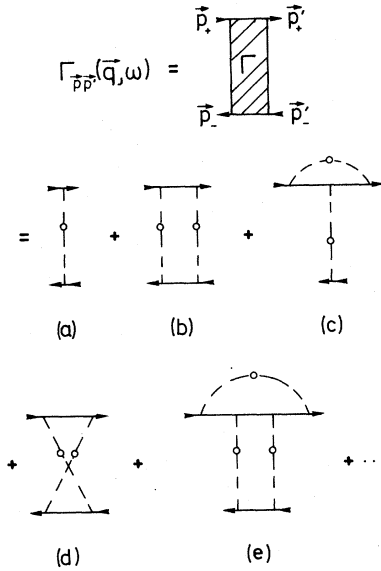(a)   (b)   (c)

(d)   (e)

FIG. 2. Typical diagrams (reducible and irreducible) contributing to the complete vertex function $\Gamma_{\vec{p}\vec{p}'}$ are shown.

tion $\Gamma_{\vec{p}\vec{p}'}$ has the general property

$$\Gamma_{\vec{p}\vec{p}'}(\vec{q},\omega) = \Gamma_{(\vec{p}-\vec{p}'+\vec{q})/2,\,(\vec{p}'-\vec{p}+\vec{q})/2}(\vec{p}+\vec{p}',\omega), \qquad (17)$$

which can be derived by time reversing, e.g., the hole line of $\Gamma_{\vec{p}\vec{p}'}$. Let us now write $\Gamma_{\vec{p}\vec{p}'}$ as $\Gamma_{\vec{p}\vec{p}'} = \Gamma^{(r)}_{\vec{p}\vec{p}'} + U_{\vec{p}\vec{p}'}$, where $\Gamma^{(r)}_{\vec{p}\vec{p}'}$ contains all reducible while $U_{\vec{p}\vec{p}'}$ contains all irreducible contributions to $\Gamma_{\vec{p}\vec{p}'}$, i.e., $U_{\vec{p}\vec{p}'}$ is the completely irreducible vertex function. In the case of time-reversal invariance, $U_{\vec{p}\vec{p}'}$ can itself be viewed to consist of two parts: $U_{\vec{p}\vec{p}'} = \overline{\Gamma}^{(r)}_{\vec{p}\vec{p}'} + \Gamma^{(i)}_{\vec{p}\vec{p}'}$. Here $\overline{\Gamma}^{(r)}_{\vec{p}\vec{p}'}$ is the set of all diagrams which are obtained when the bottom (i.e., hole) line of all $\Gamma^{(r)}$ diagrams is reversed (naturally $\overline{\Gamma}^{(r)}$ is then irreducible), while $\Gamma^{(i)}$ contains the rest of the diagrams. For example, the diagram in Fig. 2(b) belongs to $\Gamma^{(r)}$ (all diagrams to Γ^0, the diffusion propagator, except the first one [Fig. 2(a)], contribute to $\Gamma^{(r)}$), the one in Fig. 2(d) belongs to $\overline{\Gamma}^{(r)}$ and those in Figs. 2(a), 2(c), and 2(e) belong to $\Gamma^{(i)}$. Clearly, $\Gamma_{\vec{p}\vec{p}'}$ obeys the equation

$$\Gamma_{\vec{p}\vec{p}'} = U_{\vec{p}\vec{p}'} + \sum_{\vec{p}''} U_{\vec{p}\vec{p}''}\, G^{R}_{\vec{p}''_{+}} G^{A}_{\vec{p}''_{-}} \Gamma_{\vec{p}''\vec{p}'}. \qquad (18)$$

Therefore, using the definition of $U_{\vec{p}\vec{p}'}$ and (17) we can construct a (nonlinear) integral equation for $\Gamma^{(r)}$ and $\Gamma^{(i)}$:

$$\Gamma^{(r)}_{\vec{p}\vec{p}'} = \sum_{\vec{p}''} \left[\Gamma^{(r)}_{(\vec{p}-\vec{p}''+\vec{q})/2,\,(\vec{p}''-\vec{p}+\vec{q})/2}(\vec{p}+\vec{p}'') + \Gamma^{(i)}_{\vec{p}\vec{p}''} \right] G^{R}_{\vec{p}''_{+}} G^{A}_{\vec{p}''_{-}}$$
$$\times \left[\Gamma^{(r)}_{\vec{p}''\vec{p}'} + \Gamma^{(r)}_{(\vec{p}''-\vec{p}'+\vec{q})/2,\,(\vec{p}'-\vec{p}''+\vec{q})/2}(\vec{p}'+\vec{p}'') \right.$$
$$\left. + \Gamma^{(i)}_{\vec{p}''\vec{p}'} \right]. \qquad (19)$$

Given $\Gamma^{(i)}_{\vec{p}\vec{p}'}$ (using for example the approximation $\Gamma^{(i)} = U_0$) (19) can in principle be solved for $\Gamma^{(r)}$. Consequently $\Gamma_{\vec{p}\vec{p}'}$ will then possess the exact time-reversal symmetry as expressed in (17).

Turning back to the calculation of the response function $\phi_{\vec{p}\vec{p}'}$ we are now able to set up a Bethe-Salpeter equation. This equation is given by

$$\phi_{\vec{p}\vec{p}'}(\vec{q},\omega) = G^{R}_{\vec{p}_{+}} G^{A}_{\vec{p}_{-}} \left(-\frac{1}{2\pi i}\delta(\vec{p}-\vec{p}') \right.$$
$$\left. + \sum_{\vec{p}''} U_{\vec{p}\vec{p}''}(\vec{q},\omega)\phi_{\vec{p}''\vec{p}'}(\vec{q},\omega) \right). \qquad (20)$$

Inserting

$$G^{R}G^{A} = \frac{G^{A} - G^{R}}{(G^{R})^{-1} - (G^{A})^{-1}}$$
$$= -\frac{\Delta G}{\omega - \vec{p}\cdot\vec{q}/m - \Sigma^{R} + \Sigma^{A}}, \qquad (21)$$

where $\Delta G = G^{R} - G^{A}$, into (20) and multiplying the denominator of (21) to the left-hand side of the equation we rewrite the Bethe-Salpeter equation as a kinetic equation:

$$[\omega - \vec{p}\cdot\vec{q}/m - \Sigma^{R}_{\vec{p}_{+}}(E_{F}+\omega) + \Sigma^{A}_{\vec{p}_{-}}(E_{F})]\phi_{\vec{p}\vec{p}'}(\vec{q},\omega)$$
$$= \Delta G_{\vec{p}} \left(\frac{1}{2\pi i}\delta(\vec{p}-\vec{p}') - U_{\vec{p}\vec{p}''}\phi_{\vec{p}''\vec{p}'}(\vec{q},\omega) \right). \qquad (22)$$

Summing (22) on $\vec{p}$ and $\vec{p}'$ yields

$$\omega\phi(\vec{q},\omega) - q\sum_{\vec{p},\vec{p}'} (\vec{p}\cdot\hat{q}/m)\phi_{\vec{p}\vec{p}'}(\vec{q},\omega) = -N(E_{F}), \qquad (23)$$

which is equivalent to the continuity equation; in the limit $q = 0$ we recover (12). In the derivation of (23) we have made use of an important compensation mechanism between $\Sigma_{\vec{p}}$ and $U_{\vec{p}\vec{p}'}$ terms, i.e., a Ward identity, valid for all $\omega, \vec{q}$:

$$\Sigma^{R}_{\vec{p}_{+}}(E_{F}+\omega) - \Sigma^{A}_{\vec{p}_{-}}(E_{F}) = \sum_{\vec{p}'} U_{\vec{p}\vec{p}'}(\vec{q},\omega)\Delta G_{\vec{p}}. \qquad (24)$$

A proof of this Ward identity is given in Appendix A; in fact, its validity can be shown for any diagram. In (23) a new function appears, namely,

$$\phi_{j}(\vec{q},\omega) = \sum_{\vec{p},\vec{p}'} (\vec{p}\cdot\hat{q}/m)\phi_{\vec{p}\vec{p}'}(\vec{q},\omega),$$

which has the character of a current relaxation function while $\phi(\vec{q},\omega)$ is a density relaxation function.

In order to derive an equation for ϕ_{j} (i.e., a current relaxation equation) we will first expand $\phi_{\vec{p}\vec{p}'}$ in angular variables. Observing that $\mathrm{Im}G_{\vec{p}}$ is a strongly peaked function at $|\vec{p}| = p_{F}$, the width being $\gamma \ll E_{F}$ and the height γ^{-1}, the dependence of

$\phi_{\vec{p}\vec{p}'}$ on $\vec{p}$ is dominated by this peak structure through $\Delta G_{\vec{p}}$. We can therefore expand $\phi_{\vec{p}\vec{p}'}$ as

$$\sum_{\vec{p}'} \phi_{\vec{p}\vec{p}'} \simeq -[2\pi i N(E_F)]^{-1} \Delta G_{\vec{p}}$$

$$\times \sum_{\vec{p}',\vec{p}''} [1 + d(\vec{p}\cdot\hat{q})(\vec{p}''\cdot\hat{q})/p_F^2]\phi_{\vec{p}''\vec{p}'}, \quad (25)$$

where we have retained the $l = 0$ and $l = 1$ terms only. Multiplication of (22) by $\vec{p}\cdot\hat{q}/m$ and summation on $\vec{p}, \vec{p}'$ then leads to the following current relaxation equation:

$$[\omega + M(\vec{q}, \omega)]\sum_{\vec{p},\vec{p}'} (\vec{p}\cdot\hat{q}/m)\phi_{\vec{p}\vec{p}'}(\vec{q}, \omega)$$

$$-q\frac{2E_F}{md}\sum_{\vec{p},\vec{p}'} \phi_{\vec{p}\vec{p}'}(\vec{q}, \omega) = 0. \quad (26)$$

Equation (26) contains the "current relaxation kernel" $M(\vec{q}, \omega)$:

$$M(\vec{q}, \omega) = 2i\gamma + \frac{id}{2\pi N(E_F)p_F^2}$$

$$\times \sum_{\vec{p},\vec{p}'} (\vec{p}\cdot\hat{q})\Delta G_{\vec{p}} U_{\vec{p}\vec{p}'} \Delta G_{\vec{p}'}(\vec{p}'\cdot\hat{q}), \quad (27)$$

which explicitly depends on the irreducible vertex function $U_{\vec{p}\vec{p}'}$. Equations (23) and (26) form a closed set of equations that can be written as

$$\omega\phi(\vec{q}, \omega) - q\phi_j(\vec{q}, \omega) = -N(E_F),$$

$$[\omega + M(\vec{q}, \omega)]\phi_j(\vec{q}, \omega) - q\frac{2E_F}{md}\phi(\vec{q}, \omega) = 0. \quad (28)$$

Equation (28) can easily be solved for ϕ and ϕ_j. $\chi(\vec{q}, \omega)$, the density response function [see (11)], is thus found to be

$$\chi(\vec{q}, \omega) = \frac{-q^2(n/m)}{\omega^2 + \omega M - q^2(n/m\chi^T)}, \quad (29)$$

where n and m are the number density and the mass of the electron, respectively [$n/N(E_F) = 2E/d$].

Neglecting the ω^2 term in the denominator of Eq. (29) we can write

$$\chi(\vec{q}, \omega) = \chi^T(\vec{q}, 0)\frac{iD(\vec{q}, \omega)q^2}{\omega + iD(\vec{q}, \omega)q^2}, \quad (30)$$

where we have introduced a generalized, $\vec{q}$- and ω-dependent diffusion coefficient $D(\vec{q}, \omega)$:

$$D(\vec{q}, \omega) = i/[(m/n)\chi^T M(\vec{q}, \omega)], \quad (31)$$

i.e., the diffusion coefficient is essentially given by the inverse of the current relaxation kernel $M(\vec{q}, \omega)$. The dynamical conductivity $\sigma(\omega)$ and the electrical polarizability $\alpha(\omega)$ are obtained from $\chi(\vec{q}, \omega)$ by taking the limit

$$\sigma(\omega) = -i\omega\alpha(\omega) = e^2 \lim_{q\to 0} (-i\omega/q^2)\chi(\vec{q}, \omega),$$

that is,

$$\sigma(\omega) = -i\omega\alpha(\omega) = e^2\frac{n}{m}\frac{i}{\omega + M(0, \omega)}. \quad (32)$$

In the weak-coupling limit [see (14)] $U_{\vec{p}\vec{p}'}$ is given by $U_0(\vec{p} - \vec{p}')$, and one recovers the familiar result of weak-coupling transport theory, namely,

$$M(0, 0) = i/\tau$$

$$= 2\pi i n_i \sum_{\vec{p}'} \delta\left(E_F - \frac{p'^2}{2m}\right)|V(\vec{p} - \vec{p}')|^2(1 - \hat{p}\cdot\hat{p}'). \quad (33)$$

After having derived an expression for $\chi(\vec{q}, \omega)$ from a microscopic theory [i.e., (29)] it is worthwhile to note that an identical result can be obtained within a phenomenologic theory from a simple hydrodynamic model.[12] If the system is regarded as a fluid in which the random scatterers introduce effective macroscopic forces, the equation for the local density $n(\vec{r}, t)$ and the current density $\vec{j}(\vec{r}, t)$ are given by

$$\partial_t n(\vec{r}, t) + \vec{\nabla}\cdot\vec{j}(\vec{r}, t) = 0, \quad (34a)$$

$$\partial_t \vec{j}(\vec{r}, t) + \frac{1}{m}\vec{\nabla}P(\vec{r}, t)$$

$$= -\frac{1}{\tau}\vec{j}(\vec{r}, t) - \omega_0^2\int_0^t dt'\vec{j}(\vec{r}, t') + \frac{1}{m}\vec{\nabla}\mu^{ext}. \quad (34b)$$

In (34b) the first term on the right-hand side is due to the relaxation of the current with a rate $1/\tau$ (the scattering centers introduce a frictional force acting on the fluid), the second term represents a restoring force in the localized limit (with ω_0 as oscillator frequency), and the third term describes an external chemical potential. The pressure gradient can be expressed by a density gradient via $\vec{\nabla}P = (n/\chi^T)\vec{\nabla}n$. Equation (34) can now be solved for $n(\vec{q}, \omega)$ and $\vec{j}(\vec{q}, \omega)$. For

$$\chi(\vec{q}, \omega) = \delta n(\vec{q}, \omega)/\delta\mu^{ext}(\vec{q}, \omega)$$

one gets exactly the same expression as given in (29), where

$$M(0, \omega + i0) = \begin{cases} \dfrac{i}{\tau} & \text{conductor} \\[2mm] \dfrac{i}{\tau} - \dfrac{\omega_0^2}{\omega} & \text{insulator.} \end{cases} \quad (35)$$

So for the conducting case we again recover the weak-coupling result $M(0, 0) = i/\tau$, but for an insulator $M(0, \omega)$ is seen to *diverge* $\propto -1/\omega$ for $\omega \to 0$. Accordingly the conductivity is given by ($\omega < |M|$)

$$\text{Re}\sigma(\omega) = \frac{e^2 n}{\tau m}\ \frac{\omega^2}{\omega_0^4 + \omega^2/\tau^2}\ . \tag{36}$$

For the insulator ($\omega_0 \neq 0$) we have $\text{Re}\sigma(\omega)$ $= e^2 n (\tau m \omega_0^4)^{-1}\omega^2 \sim \omega^2$ so that the dc conductivity is zero, while for the conductor ($\omega_0 = 0$) it is finite [$\text{Re}\sigma(0) = e^2 \tau n/m$], whereas the static polarizability $\alpha(0)$ is finite for the insulator case and infinite for the conductor.

By means of the static susceptibility $\chi(\vec{q}, 0)$ we can now derive an expression for the localization length r_0 of the system in the localized regime[8]

$$\chi(\vec{q}, 0) = \chi^T(0, 0)\frac{r_0^2 q^2}{1 + r_0^2 q^2}\ . \tag{37}$$

From (29) together with (35) we find r_0 $= (m\omega_0^2 \chi^T/n)^{-1/2}$, i.e., the localization length is inversely proportional to the root of the restoring force. It should be reiterated that the $1/\omega$ divergence of $M(0, \omega)$ for small ω [rather than the disappearance of the conductivity $\sigma(\omega)$] is the very signature of localization.

III. INFRARED DIVERGENCIES OF THE RELAXATION KERNEL $M(\vec{q},\omega)$

In the preceding section we have shown how both microscopic theory and a simple hydrodynamic model lead to identical expressions for the density response function $\chi(\vec{q}, \omega)$ for the system under consideration. Furthermore, we have pointed out how the physics of the problem is essentially contained in a current relaxation kernel $M(\vec{q}, \omega)$ for which the hydrodynamic model finds that it stays finite for $\omega, \vec{q} = 0$ for a conducting system while it diverges $\propto - 1/\omega$ in this limit (infrared divergence) in the insulating regime. In this section we will show that such divergencies of $M(\vec{q}, \omega)$ naturally exist for a system of noninteracting electrons in a random impurity potential for $d \leqslant 2$ dimensions even for arbitrarily weak disorder. For this we will proceed in two steps:

(i) It will be shown that the perturbation series for $M(\vec{q},\omega)$ contains terms diverging like $1/\sqrt{\omega}$ or $\ln\omega$ for small ω in $d = 1$ or $d = 2$, respectively.

(ii) Then we will show how a self-consistent generalization for $M(\vec{q}, \omega)$ indeed leads to the overall $M \propto - 1/\omega$ behavior for $d \leqslant 2$ and arbitrarily weak disorder.

The relaxation kernel $M(\vec{q}, \omega)$ as given by (27) is mainly determined by the irreducible vertex function $U_{\vec{p}\vec{p}'}$. A divergence of M and hence localization is only possible when the diagrammatic perturbation theory breaks down. Therefore we have to search for contributions to $U_{\vec{p}\vec{p}'}$ which in turn lead to the divergence in M. In the preceding section II we have already seen how particle conservation is responsible for the cancellation of

the ($\omega, \vec{q}$)-independent terms in the sum of particle-hole ladder diagrams, giving rise to a typical diffusion pole for the (bare) diffusion propagator $\Gamma^0(\vec{q}, \omega)$. It is clear that the q integral over any such diffusion denominator (i.e., $\omega + iDq^2$) will diverge in the limit $\omega \to 0$ for dimensions $d \leqslant 2$:

$$\int dq\ \frac{q^{d-1}}{\omega + iD_0 q^2}\ \underset{\omega \to 0}{\propto}\ \begin{cases} \dfrac{1}{\sqrt{\omega}}\ , & d = 1 \\[2ex] \ln\omega, & d = 2\ , \end{cases} \tag{38}$$

where for $d = 2$ an appropriate cutoff momentum for large q has to be introduced. It is this very infrared singularity in the density propagator that introduces divergencies into perturbation theory. Let us therefore first discuss and analyze diagrams to $M(\vec{q}, \omega)$ containing a diffusion propagator Γ^0 arising from summation of particle-hole ladder diagrams (Fig. 3). The simplest diagrams contributing to $U_{\vec{p}\vec{p}'}$ to lowest order in γ/ E (i.e., the simplest irreducible diagrams with Γ^0) are shown in Fig. 4. Note that the second-order crossed diagram to U^D appears twice. This is, however, of no consequence because the over-counted diagram (which is finite) only yields a higher-order correction to an otherwise divergent expression as can be seen below. The contribution to M from these diagrams is

$$M^D(\vec{q}, \omega) = -\frac{d}{p_F^2}\ U_0 \sum_{\vec{k}}\ \frac{q^2 + (\vec{k}\cdot\hat{q})^2}{\omega + iD_0 k^2}$$

$$\underset{\omega \to 0}{\approx}\ \frac{q^2}{2p_F^2}\ \frac{i}{\tau}\ F_d(\omega),\quad d = 1, 2 \tag{39}$$

where $F_1(\omega) = (2/\pi)(i/\omega\tau)^{1/2}$ and $F_2(\omega) = 2\pi E\tau)^{-1}\ln(1/ \omega\tau)$. Here the momentum dependence of U_0 has been neglected and the superscript D at M indicates that M^D is the lowest-order diffusion contribution to M. Note that for $q = 0$ M^D is finite for $\omega \to 0$, i.e., there is only a divergence in M^D for
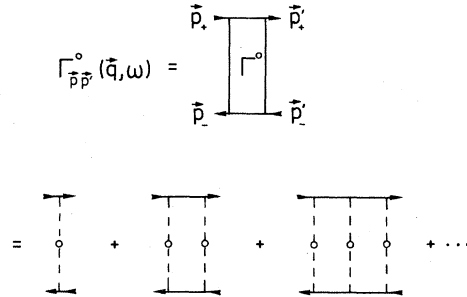
$$\Gamma^0_{\vec{p}\vec{p}'}(\vec{q},\omega)\ =$$

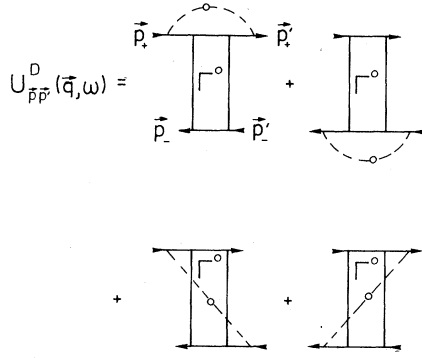FIG. 3. Diffusion propagator $\Gamma^0_{\vec{p}\vec{p}'}$, which is the sum of all particle-hole ladder diagrams, is shown.

FIG. 4. The four lowest-order diagrams of the irreducible vertex $U^D_{\vec{p}\vec{p}'}$, with respect to the divergence of Γ^0 for $\omega \to 0$ are shown.

FIG. 5. $\Lambda^0_{\vec{p}\vec{p}'}$, which is the sum of all maximally crossed diagrams, is shown.

$q \neq 0$. This is due to the fact that for $q = 0$ $U_{\vec{p}\vec{p}'}$ separates into two parts, one depending only on $\vec{p}$, the other one only on $\vec{p}'$. As the Green's functions are even in the momentum, the (odd) vertex parts $(\vec{p} \cdot \hat{q})$ and $(\vec{p}' \cdot \hat{q})$ in (27) consequently make the integral vanish. Note that if one replaces the diffusion propagator in (39) in terms of the density relaxation functions ϕ by means of (11) and (30) one obtains an expression for M which is identical to the one derived by Götze[8] in the mode-coupling theory.

A natural question is then whether there exist divergencies in $M(0, \omega)$ due to a diffusion pole at all. We have found a mathematically exact answer to this question which is formulated in the following theorem.

Theorem. Any diagram for the q-independent current relaxation kernel $M(0, \omega)$ or the diffusion coefficient $D(0, \omega)$ (Refs. 6 and 13) containing a (bare) diffusion propagator Γ^0 belongs to a uniquely defined class of diagrams, which can systematically be generated and whose sum of divergent contributions is zero.

The proof is given in Appendix B. This implies that the usual diffusion mechanism described by a diffusion propagator Γ^0 cannot lead to divergent contributions in $M(0, \omega)$ and, hence, that localization cannot be due to particle-hole diffusional scattering in $d \leq 2$.

There is, however, still another scattering mechansim which *can* lead to infrared divergencies of M even for $q = 0$. Abrahams et al.[5] were the first to note that in the case of time-reversal invariance the diffusion pole of Γ^0 can be transferred to the particle-particle channel by means of a $2k_F$ scattering mechanism. They found that the sum $\Lambda^0_{\vec{p}\vec{p}'}(\vec{q}, \omega)$ of all maximally crossed diagrams (Fig. 5) is given by
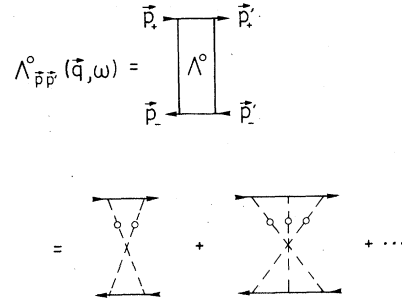
$$\Lambda^0_{\vec{p}\vec{p}'}(\vec{q}, \omega) = \frac{2i\gamma U_0}{\omega + iD_0(\vec{p}+\vec{p}')^2} \quad \text{for } \vec{p} \simeq -\vec{p}'. \quad (40)$$

These diagrams can be viewed as obtained from those for Γ^0 when the hole line of every diagram of Γ^0 is reversed (such a reversal is only permitted in the presence of time-reversal invariance). Using the notation previously introduced this implies $\Lambda^0_{\vec{p}\vec{p}'}(\vec{q}, \omega) = \overline{\Gamma}^0_{\vec{p}\vec{p}'}(\vec{q}, \omega)$. The diagrams for $\Lambda^0_{\vec{p}\vec{p}'}$ are already particle-hole irreducible and therefore belong to $U_{\vec{p}\vec{p}'}$. Λ^0 yields an infrared divergent contribution to M even at $q = 0$:

$$M^{2k_F}(0, \omega) = -2U_0 \sum_{\vec{k}} \frac{1}{\omega + iD_0 k^2} \underset{\omega \to 0}{\simeq} \frac{i}{\tau} F_d(\omega),$$
$$(41)$$

where $F_d(\omega)$ has been defined below (39). It should be noted that time-reversal invariance will be invalidated by any magnetic field (either an external field or one generated by magnetic impurities leading to spin-flip scattering).[14] Therefore such fields will remove the infrared divergence (see below), because a time-reversal invariance-breaking term i/τ_s (where τ_s is the spin-flip scattering time) enters the theory via the replacement $\omega \to \omega + i/\tau_s$ removing the singularity at $\omega \to 0$.

We have now completed our first task, namely, to show that there exist infrared divergent contributions to $M(\vec{q}, \omega)$ at all. This is not enough, however. It should be remembered that the diffusion coefficient $D(\vec{q}, \omega)$ is related to M by $D(\vec{q}, \omega) = D_0[(i/\tau)/M(\vec{q}, \omega)]$. Therefore the (dressed) diffusion coefficient can only be represented by the diffusion *constant* D_0 as long as $(i/\tau)/M(\vec{q}, \omega)$ does not change too much. As we have found that $M(\vec{q}, \omega)$ diverges for $\omega \to 0$, this condition is certainly not fulfilled any longer and therefore we have to replace D_0 by the full diffusion coefficient $D(\vec{q}, \omega)$ in the diffusion denominator of (39) and (41). This replacement in the

two equations [which is permitted because the pole structures of Γ^0 and Λ^0 are related via (17)] then leads to a self-consistent equation for $M(0, \omega)$:

$$M(0, \omega) = \frac{i}{\tau} - 2U_0 \sum_{|\vec{k}| < k_0} \frac{1}{\omega + i/\tau_s - k^2 D_0 \tau^{-1}/M(0,\omega)}$$

(42)

Here we have introduced an upper cutoff for $d = 2$ of the order of p_F and the time-reversal invariance-breaking term i/τ_s has explicitly been included.

Before we further discuss (42), describing $2k_F$ scattering, and other possible divergent contributions due to multiple Λ^0 poles, it is instructive to discuss the consequences of the self-consistent generalization for the diffusion propagator Γ^0. In Ref. 15 $M(\vec{q}, \omega)$ has been calculated within a mode-coupling approximation in a memory function approach. The divergence found within this theory is identical to the one we found in (39) corresponding to the four diagrams with Γ^0 in Fig. 4. Although (39) only diverges for $q \neq 0$ a self-consistent generalization of (10) [which yields the $M(\vec{q}, \omega)$ of Ref. 8] within the mode-coupling theory will transfer the $q \neq 0$ divergence even to $M(0, \omega)$. This would have implied that indeed in the weak-coupling limit both the usual diffusional scattering *and* the $2k_F$ scattering lead to a divergence of M and thus to localization. However, our diagrammatic analysis permits us to identify the diagrams corresponding to the self-consistent generalization of Ref. 15. In Fig. 6(b) we show a typical diagram generated from the initial one in Fig. 6(a) by means of the self-consistency. The class of diagrams thus constructed leads to the $q = 0$ divergence of Ref. 15. Employing the rules for cancellation of diagrams which we have worked out (see Appendix B), we can immediately construct the diagram [Fig. 6(c)] which cancels the one in Fig. 6(b) but which is *not* generated by the self-consistent generalization (in the case of two interaction lines crossing Γ^0 we simply have to exchange the endpoints of those lines on the right of Γ^0). In this way we can cancel *all* diagrams of the self-consistent generalization of Ref. 15, i.e., a divergence due to Γ^0 does not exist.

We now return to the $2k_F$ scattering mechanism and Eq. (42). In contrast to the diagrammatic approaches of Gorkov *et al.*[6] and Khmelnitskii[13] who investigated the conductivity [i.e., the diffusion coefficient $D(\vec{q}, \omega)$ itself] and who employed the complete vertex function $\Gamma_{\vec{p}\vec{p}'}$, the important quantity for us is the irreducible vertex function $U_{\vec{p}\vec{p}'}$, which determines $M(\vec{q}, \omega)$. In Refs. 6 and 13 contributions to $D(\vec{q}, \omega)$ for $d = 2$ of the order $[(1/E\tau)\ln(1/\omega\tau)]^n$ for $n \geq 2$ have been discussed
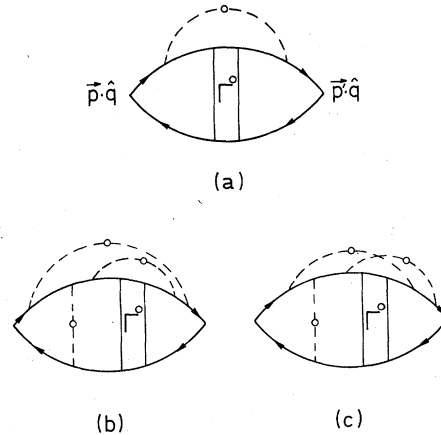

(a)

(b)   (c)

FIG. 6. (a) One of the four lowest-order divergent diagrams for $M(\vec{q}, \omega)$ containing a diffusion propagator Γ^0 is shown; (b) a typical diagram for $M(\vec{q}, \omega)$ as is generated from the lowest-order diagrams by the self-consistent generalization; (c) diagram which cancels the one in (b) but is not generated by the self-consistent generalization.

[the following discussion is also valid for $d = 1$; in this case $\ln(1/\omega\tau)$ has to be replaced by $1/\sqrt{\omega\tau}$. For $n = 2$ cancellation of all diagrams has explicitly been shown,[6] while the disappearance for $n > 2$ was made plausible by means of a renormalization-group equation.[6,13] Bearing in mind that $U_{\vec{p}\vec{p}'}$ only makes up a subset of those diagrams of $\Gamma_{\vec{p}\vec{p}'}$ which contribute to this order, we are in a different position altogether. In our case, contributions of $[(1/E\tau)\ln(1/\omega\tau)]^n$ will certainly not vanish—in fact, they must necessarily exist because (42) can be viewed as a resummation of diagrams of *any* order in n (for $d \leq 2$) *and* the coupling constant. This can be shown as follows: In general, a diagram with n Λ^0 poles not only contributes to order $[\ln(1/\omega\tau)]^n$ but also to $[\ln(1/\omega\tau)]^{n-1}$, etc. (with possibly a higher power of the coupling constant as prefactor) when one expands the Green's functions in the (small) momenta of each pole. To investigate this we have considered the complete (reducible and irreducible) classes of diagrams, as classified by n, the number of Λ^0 poles in the diagrams. Now we have made two assumptions:

(i) To lowest order in $1/E\tau$ all contributions to the complete vertex function of order $[\ln(1/\omega\tau)]^n$, $n \geq 2$, vanish as argued in Refs. 6 and 13.

(ii) The contributions of order $[\ln(1/\omega\tau)]^m$, $m < n$, from a diagram with n Λ^0 poles can be neglected compared to those from diagrams with exactly m Λ^0 poles because they are of higher order in the coupling constant.

With these assumptions we have been able to show that the *whole* class of irreducible diagrams of order n is equal to $(-1)^{n+1}$ times the reducible diagram where n Λ^0 poles are arranged in parallel, like rungs of a ladder. The latter diagrams can easily be summed up, but the result is different from what we get from (40) in that it does not diverge like $-1/\omega$ as it should. Therefore we expect assumption (ii) to be wrong. However, this immediately leads to the conclusion that non-leading divergent terms (in regard to their coupling-constant dependence) as generated by the self-consistent equation are equally important.

Besides diagrams which contribute $[\ln(1/\omega\tau)]^n$ terms and which necessarily must exist in our theory, we have discovered one special class of "superdiverging" diagrams which have the general structure displayed in Fig. 7(a). In these diagrams two Λ^0 propagators cross each other, ending nearest to the left and right vertices. In order for these diagrams to be permitted at all, there has to be some diagrammatic insertion in the middle of the diagram. Owing to this structure both Λ^0 poles have the *same* momentum dependence, i.e., the integrand of $M(\vec{q}, \omega)$ contains a denominator $(\omega + iD_0 k^2)^2$, which diverges like $\omega^{-3/2}$ in $d=1$ and ω^{-1} in $d=2$. We are able to show, however, that these superdiverging diagrams cancel exactly due to particle number conservation (see Appendix C).

Even if there are no infrared divergencies in individual terms of the perturbation expansion (e.g., as in $d \geqslant 3$) there will in any case exist a critical value of the coupling constant for which the total sum of the perturbation expansion diverges, so that even in this case $M \propto -1/\omega$. In other words, the density relaxation function ϕ behaves like $\phi(\vec{q}, \omega) \propto f(\vec{q})/\omega$ for small ω, where f is some function of $\vec{q}$. The simplest diagrams contributing to this divergence are again those
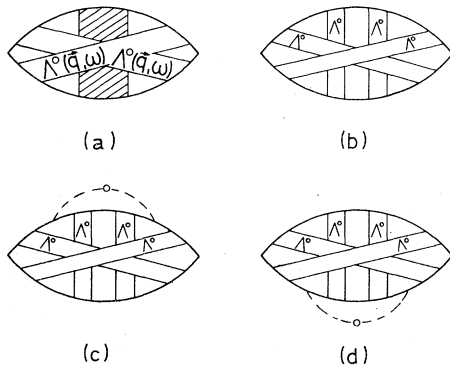

(a)   (b)

(c)   (d)

FIG. 7. (a) General structure of the "superdiverging" diagrams for $M(0, \omega)$. In (b)–(d) a typical group of diagrams which cancel each other are shown (see text).

depicted in Fig. 4, which have been shown to give rise to a contribution M^D, (39), to the relaxation kernel. Indeed a self-consistent generalization of (39) for $M(0, \omega)$ as derived by Götze[8] in a mode-coupling theory yields an Anderson transition in $d=3$. We believe that the application of these ideas to the Anderson transition itself is not invalidated by our finding that divergent contributions to $M(0, \omega)$ generated by diffusion poles cancel.

IV. RESULTS

The results of the theory as presented here are contained in (42), an implicit equation for the relaxation kernel $M(0, \omega)$. For $d > 2$ there are no infrared divergences contributing to M and (42) gives the same result for both $D(0, \omega)$ and D_0, the diffusion constant [in fact, although in this case the arguments leading to the self-consistent generalization are still valid they are also unnecessary because $M(0, \omega)$ is always finite: The self-consistency therefore does not change the final result]. So for $d > 2$ the solution is given by $M(0,0) = i/\tau$ for small impurity concentration, i.e., the system is conducting and according to (36) the conductivity is given by $\mathrm{Re}\sigma(0) = e^2\tau n/m = \mathrm{const}$. For $d \leqslant 2$, however, (42) will lead to a diverging $M(0, \omega)$ if $i/\tau_s = 0$, implying time-reversal invariance. The self-consistent solution indeed yields $M(0, \omega) = i/\tau - \omega_0^2/\omega$, which corresponds to an insulator (i.e., localized solution) with

$$\omega_0^2 = \begin{cases} \left(\dfrac{\pi}{2} E_F\right)^2 \lambda^2, & d=1 \\[2ex] 2(E_F x_0)^2 \exp(-1/\lambda), & d=2 \end{cases} \tag{43}$$

where $\lambda = n n_i [V(q=0)/E_F]^2$ is a dimensionless coupling parameter $[\lambda = (2\pi E_F \tau)^{-1} \ll E_F]$ and x_0 is a dimensionless cutoff parameter. From (32) we find that the static electrical polarizability $\alpha(0)$ and the dynamical conductivity $\mathrm{Re}\sigma(\omega)$ are given by $\alpha(0) = (e^2 n/m)/\omega_0^2$ and

$$\mathrm{Re}\sigma(\omega) = \begin{cases} \dfrac{e^2}{\tau} \dfrac{n}{m} \left(\dfrac{\pi}{2} E_F\right)^{-4} \dfrac{\omega^2}{\lambda^4}, & d=1 \\[2ex] \dfrac{e^2}{4\tau} \dfrac{n}{m} (E_F x_0)^{-4} \omega^2 \exp(2/\lambda), & d=2 \end{cases} \tag{44}$$

respectively. Note, that for $d=1$, $\alpha(0)$ leads to a dielectric constant $\epsilon_0 = 4\pi\alpha(0)$, i.e., $\epsilon_0 = 32e^2(p_F/m)\tau^2$, which agrees with the exact results[16,17] apart from a factor[17] of $\zeta(3) \simeq 1.20$. The conductivity in (44) for $d=1$ can be rewritten as

$$\mathrm{Re}\sigma(\omega) = (8/\pi)e^2(p_F/m)\tau^3 \omega^2 ,$$

which again agrees with the exact result of Ref. 17 apart from the additional $(\ln\omega)^2$ term due to level repulsion, which cannot be obtained within the present theory.

For $d=2$, $\text{Re}\sigma(\omega)$ and $\alpha(0)$ are dominated by the exponential dependence on the inverse of the coupling parameter λ, i.e., $\alpha(0)$ becomes exponentially large for small disorder. It should be pointed out that in calculating $M(0,\omega)$ the central quantity we have determined is $\omega_0=(2E_F/dm)^{1/2}r_0^{-1}$, i.e., the inverse localization length. As far as the localization length r_0 itself is concerned we therefore find $r_0\sim 1/\lambda$ for $d=1$ and $r_0\sim\exp(1/2\lambda)$ for $d=2$, i.e., for $d=2$ the localization length also becomes exponentially large.

In the case of spin-flip scattering $(i/\tau_s\neq 0)$ the present theory yields localization neither for $d=2$ nor for $d=1$ in the weak-coupling limit. To our knowledge, proofs for localization in $d=1$ have so far never considered the effect of spin-flip scattering.

In Ref. 12 we had already mentioned that inelastic scattering effects at finite temperatures can be introduced into the present theory by the replacement $\omega\to\omega+i/\tau_{\text{inel}}$, where τ_{inel} is the inelastic scattering time. In the weak-coupling limit the lowest-order corrections to $M=i/\tau$ are then $(\tau_{\text{inel}})^{1/2}$ and $\ln\tau_{\text{inel}}$ for $d=1$ and $d=2$, respectively. At low temperatures this implies a temperature dependence $T^{-1/2}$ for $d=1$ assuming $1/\tau_{\text{inel}}\propto T$ and $\ln T$ for $d=2$, for the resistance of metal wires and films containing impurities. Experimental studies of such systems have been performed[18-20] and seem to have found the above temperature dependence, which has been associated with the $2k_F$ scattering mechanism by Anderson *et al.*[21]

V. CONCLUSION

A diagrammatic theory for the density response function of a system of independent particles moving in a random potential at $T=0$ has been presented for dimensions $d\leq 2$. For this the Bethe-Salpeter equation for the irreducible vertex function has been rewritten as a kinetic equation containing the current relaxation kernel $M(\vec{q},\omega)$ which is essentially the inverse diffusion coefficient. We have investigated the infrared divergent contributions to $M(0,\omega)$ and have found that such divergencies are never due to simple diffusional scattering (i.e., particle-hole ladder diagrams) because of a new cancellation mechanism. Therefore only the $2k_F$ scattering mechanism[5] can generate divergent contributions to $M(0,\omega)$ provided time-reversal invariance is valid. Furthermore, we have shown how a self-consistent generalization of $M(0,\omega)$ leads to a singular behavior of $M(0,\omega)\propto -1/\omega$ for

$\omega\to 0$ in $d\leq 2$ in the weak-coupling limit. Just as for a simple hydrodynamic model for the system under consideration, this result implies a dynamical conductivity $\text{Re}\sigma(\omega)\propto\omega^2$ and a finite static polarizability for arbitrarily weak disorder. Correspondingly the localization lengths for $d=1,2$ are found to be finite, although for $d=2$ it becomes exponentially large. Hence for $d=1$ we essentially recover the (exact) results of Abrikosov and Ryshkin[17] by means of a comparatively short derivation which offers a transparent physical interpretation. On the other hand, the explicit results for $d=2$ for the frequency-dependent conductivity had not been derived before. Finally, it should be pointed out that in our view the main result of this paper is the theoretical unification of mode-coupling concepts with a standard diagrammatic analysis as discussed in Sec. III rather than the mere calculation of the $\sigma(\omega)$, etc., which is just one result of an application of this theory. Indeed, the kinetic equation (22) together with the self-consistent generalization of $M(\vec{q},\omega)$ provide a novel framework for the calculation of transport properties of disordered systems.

ACKNOWLEDGMENT

APPENDIX A: THE WARD IDENTITY

In the derivation of (23) and (26) we made use of a Ward identity given in (24), valid for all $\omega,\vec{q}$, which we will prove now. The retarded self-energy is given by

$$\Sigma_{\vec{p}_+}^R(E_F+\omega)=\sum_{\text{Diagr. }\{n\}}\ \sum_{\{\vec{q}_i\}}U_1U_2\cdots U_n$$

$$\times G_{\vec{p}_+-\vec{q}_1}^R G_{\vec{p}_+-\vec{q}_2}^R\cdots G_{\vec{p}_+-\vec{q}_N}^R,$$

(A1)

where the U_i are the (momentum-independent) bare vertices describing the ith interaction line. Here the first sum on the right-hand side (rhs) goes over all classes of skeleton diagrams classified by n, the number of interaction lines and the second one sums up all n intermediate momenta of a diagram with n interaction lines (such a skeleton diagram consists of $N=2n-1$ Green's functions depending on different combinations of those n momenta). The advanced self-energy is defined analogously with index A, etc. The difference between both self-energies hence is

$$\Delta\Sigma_{\vec{p}} = \sum_{\text{Diagr. } \{n\}} \sum_{\{\vec{q}_i\}} U_1 U_2 \cdots U_n$$

$$\times \{G_1^R G_2^R \cdots G_N^R - G_1^A G_2^A \cdots G_N^A\},$$

$$(A2)$$

where $\Delta\Sigma_{\vec{p}} = \Sigma_{\vec{p}_+}^R(E_F + \omega) - \Sigma_{\vec{p}_-}^A(E_F)$ and where the momentum indices of the Green's function have been abbreviated for convenience. The difference in curly brackets on the rhs of (A2) can be rewritten by means of the mathematical identity

$$X_1 X_2 \cdots X_{N-1} X_N - Y_1 Y_2 \cdots Y_{N-1} Y_N = X_1 X_2 \cdots X_{N-1} \Delta X_N + X_1 X_2 \cdots \Delta X_{N-1} Y_N$$

$$+ \cdots + X_1 \Delta X_2 \cdots Y_{N-1} Y_N + \Delta X_1 Y_2 \cdots Y_{N-1} Y_N,$$

$$(A3)$$

where $\Delta X_i \equiv X_i - Y_i$. We now identify the X_i and Y_i with G_i^R and G_i^A, respectively, and perform a transformation of momenta so that all $\Delta G_i = G_{\vec{q}_{i+}}^R - G_{\vec{q}_{i-}}^A$ depend on the same momentum. Then (A2) becomes

$$\Delta\Sigma_{\vec{p}} = \sum_{\text{Diagr. } \{n\}} \sum_{\{\vec{q}_i\}} U_1 U_2 \cdots U_n \{G_1^R G_2^R \cdots G_{N-1}^R \Delta G_N^R + G_1^R G_2^R \cdots \Delta G_{N-1} G_N^A$$

$$+ \cdots + G_1^R \Delta G_2 \cdots G_{N-1}^A G_N^A + \Delta G_1 G_2^A \cdots G_{N-1}^A G_N^A\}$$

$$= \sum_{\vec{p}'} U_{\vec{p}\vec{p}'}(\vec{q}, \omega) \Delta G_{\vec{p}'} .$$

$$(A4)$$

It is not difficult to see that the second equal sign in (A4) holds true, because the procedure as described just constructs *all* diagrams of the irreducible vertex part $U_{\vec{p}\vec{p}'}$. One can visualize this by applying the following "recipe":

(i) Take any skeleton diagram of the self-energy (we assume the Green's functions to be retarded).

(ii) Start from the right to remove exactly *one* Green's-function line of the diagram and "flip" the rest of the diagram on the right down to the hole line.

(iii) Proceed through the whole diagram from right to left.

For an example we start with the self-energy diagram in Fig. 8(a) (the *only* proper diagram with two interaction lines):

$$\Delta\Sigma_{\vec{p}}^{(2)} = \sum_{\vec{p}_1,\vec{p}_2} U(\vec{p}_1) U(\vec{p}_2) (G_{\vec{p}_+-\vec{p}_1}^R G_{\vec{p}_+-\vec{p}_1-\vec{p}_2}^R G_{\vec{p}_+-\vec{p}_2}^R - G_{\vec{p}_--\vec{p}_1}^A G_{\vec{p}_--\vec{p}_1-\vec{p}_2}^A G_{\vec{p}_--\vec{p}_2}^A)$$

$$= \sum_{\vec{p}_1,\vec{p}_2} U(\vec{p}_1) U(\vec{p}_2) (G_{\vec{p}_+-\vec{p}_1}^R G_{\vec{p}_+-\vec{p}_1-\vec{p}_2}^R \Delta G_{\vec{p}-\vec{p}_2} + G_{\vec{p}_+-\vec{p}_1}^R \Delta G_{\vec{p}-\vec{p}_1-\vec{p}_2} G_{\vec{p}_--\vec{p}_2}^A + \Delta G_{\vec{p}-\vec{p}_1} G_{\vec{p}_--\vec{p}_1-\vec{p}_2}^A G_{\vec{p}_--\vec{p}_2}^A)$$

$$= \sum_{\vec{p},\vec{p}'} [U(\vec{p}_1) U(\vec{p}-\vec{p}') G_{\vec{p}_+-\vec{p}_1}^R G_{\vec{p}_+-\vec{p}_1}^R + U(\vec{p}_1) U(\vec{p}-\vec{p}'-\vec{p}_1) G_{\vec{p}_+-\vec{p}_1}^R G_{\vec{p}_-+\vec{p}_1}^A$$

$$+ U(\vec{p}-\vec{p}') U(\vec{p}_2) G_{\vec{p}_--\vec{p}_2}^A G_{\vec{p}-\vec{p}_2}^A] \Delta G_{\vec{p}'}$$

$$= \sum_{\vec{p}'} U_{\vec{p}\vec{p}'}^{(2)}(\vec{q}, \omega) \Delta G_{\vec{p}'} .$$

$$(A5)$$

Comparing the expressions in the next to last equation of (A5) with those for the diagrams in Figs. 8(b)–8(d) we can verify that we have constructed all possible contributions to $U_{\vec{p}\vec{p}'}$ with two interaction lines. Conversely one can see that every diagram for $U_{\vec{p}\vec{p}'}$ is generated from a self-energy diagram—for this one just has to reverse the sequence of steps of the recipe. In this way (24) can be proven diagram by diagram.

APPENDIX B: PROOF OF THE CANCELLATION THEOREM FOR DIAGRAMS CONTAINING Γ^0

We are now going to prove the theorem formulated in Sec. III about the cancellation of all divergent contributions of diagrams to $M(0, \omega)$ or $D(0, \omega)$ (Refs. 6 and 13) containing a (bare) diffusion propagator Γ^0. To do this we should first point out the following:
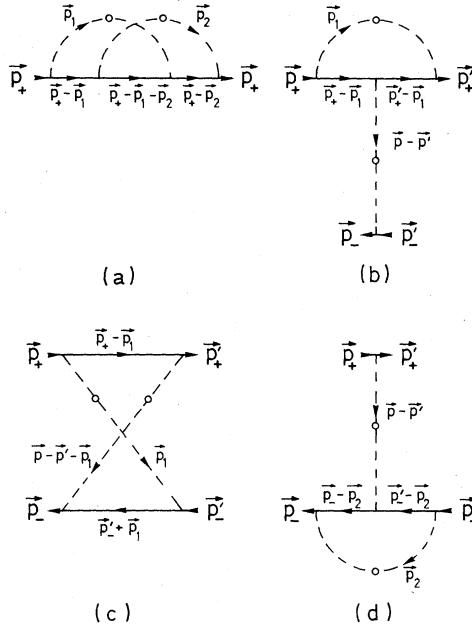
(a)   (b)

(c)   (d)

FIG. 8. (a) The only skeleton self-energy diagram with two interaction lines is shown; (b)–(d) all possible contributions to the irreducible vertex function $U_{\vec{p}\vec{p}'}$ are shown as generated from the self-energy diagram (see text).

(i) As we are only interested in divergent contributions to $M(0, \omega)$ due to the integral over Γ^0 (i.e., over the denominator $\omega + iDk^2$) we set $\omega = 0, k = 0$ everywhere else in the integrand of $M(0, \omega)$.

(ii) In this case the sum of all momenta of interaction lines going from one side of the diagram to the other (i.e., crossing Γ^0) is zero.

If there are n such interaction lines it is convenient to choose the corresponding momenta as $-\vec{q}_1, \vec{q}_1 - \vec{q}_2, \vec{q}_2 - \vec{q}_3, \ldots, \vec{q}_{n-1} - \vec{q}_n, \vec{q}_n$; in particular, for $n = 1$ the momentum of the (single) line is zero and for $n = 2$ the momenta are $\pm\vec{q}_1$. The diffusion propagator divides every diagram into two parts and in everything that follows we only need to consider *one* side of a diagram (which we choose to be the rhs) containing a single $\vec{p} \cdot \hat{q}$ vertex [see Fig. 9(a)]. The other side of the diagram [in our case the left-hand side (lhs)] can be *arbitrarily* complicated (if it contains further Γ^0 and Λ^0 poles the cancellation mechanism removes at least the highest order divergent contribution) because this does not change the fact that the sum of the momenta of the lines crossing Γ^0 is zero. Also observe that the inversion of one side of a diagram ("turning it upside down") corresponds to interchange of particle-hole lines. This is equivalent to introducing a minus sign into the $(\vec{p} \cdot \hat{q})$ vertex and exchanging $G_{\vec{p}}$ by $G_{\vec{p}}^*$ and vice versa. For example, the half-diagram
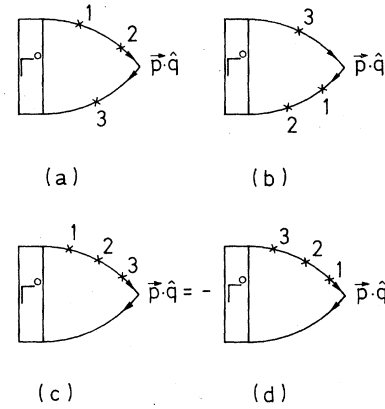

FIG. 9. rhs of several diagrams for $M(0, \omega)$ containing Γ^0 are shown. The crosses and numbers represent different endpoints of interaction lines coming from the lhs and which are crossing Γ^0 (see text).

in Fig. 9(b) is equal to the negative complex conjugate of that in Fig 9(a). Hence, one side of a half-diagram plus the inverted one gives $2i$ times the imaginary part of that side. It is also easy to see that if all interaction lines end on *either* the particle *or* the hole line of one side, as in Fig. 9(c), the half-diagram where the sequence of the endpoints of the lines is interchanged [Fig. 9(d)] gives exactly the negative of the first one. This is so because inversion of this sequence is equivalent
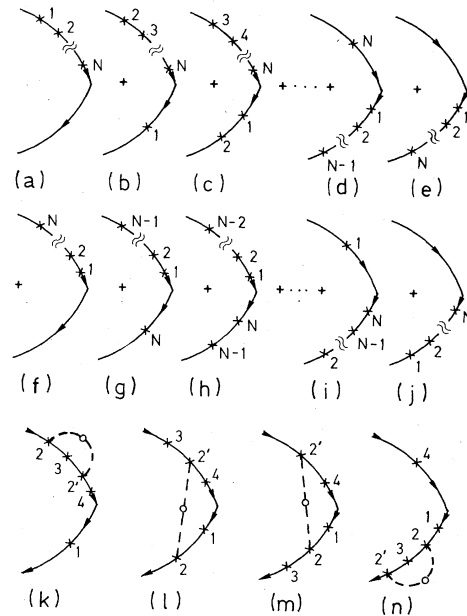

FIG. 10. Illustration of the explicit generation of the class of diagrams for $M(0, \omega)$ containing Γ^0 which cancel each other. Only rhs of diagrams are shown; the Γ^0 propagators have not been drawn (see text).

to the change $\vec{p} \rightarrow -\vec{p}$ leading to an identical momentum dependence of the Green's functions as before but with an over all minus sign due to the $(\vec{p} \cdot \vec{q})$ vertex. Therefore these types of diagrams cancel each other.

We are now going to show that any diagram with n interaction lines crossing Γ^0 and arbitrary vertex corrections is part of a class of diagrams which can systematically be generated and whose sum is exactly zero. Imagine a diagram with n such lines and, in addition, m vertex corrections on the rhs. Altogether there will be $N = n + 2m$ starting and end points, respectively, of interaction lines on the rhs of the diagram. The class is generated as follows (Fig. 10).

(i) First, all N points are supposed to lie on the particle line of the rhs [Fig. 10(a)].

(ii) Now the points are brought down to the hole line one by one in a cyclic way [Fig. 10(b)–10(d)]

until they are all on the bottom line [Fig. 10(e)] (starting and end points of vertex corrections always stay connected by their interaction line).

(iii) Now the sequence of points in Fig. 10(a) is reversed and the same procedure is done again [Figs. 10(f)–10(j)].

The last step can also be viewed as the inversion of the first $N+1$ half-diagrams [e.g., Fig. 10(i) is the inverted form of Fig. 10(b), etc.]. We know already that the half-diagrams that have been constructed in that last step are just the negative complex conjugates of the ones generated in the first two steps. Furthermore, we know that the diagrams in Figs. 10(a) and 10(f) and 10(e) and 10(j) just have their sequence of points inverted, so they are opposite in sign and cancel each other. Therefore we do not have to consider them any further. The sum S of the remaining $2(N-1)$ diagrams is

$$S = 2i \sum_{\{\vec{q}_i\}} (\vec{p} \cdot \vec{q}) \operatorname{Im}(G_{\vec{p}}) \operatorname{Im}(|G_1|^2 G_2 \cdots G_N + G_1^* |G_2|^2 \cdots G_N + \cdots + G_1^* G_2^* \cdots |G_{N-1}|^2 G_N + G_1^* G_2^* \cdots |G_N|^2).$$

(B1)

Observing that $\Delta G_{\vec{p}} = G_{\vec{p}} - G_{\vec{p}}^* = 2i \operatorname{Im}(G_{\vec{p}})$ and therefore

$$\Delta G_{\vec{p}} = -2i\gamma |G_{\vec{p}}|^2$$

(B2)

and $\operatorname{Im}(iz) = \operatorname{Re} z$ for any z, we can substitute the $|G_i|^2$ in (B1) by $(i/2\gamma)\Delta G_i$. Therefore

$$S = (i/\gamma) \sum_{\vec{p}} (\vec{p} \cdot \vec{q}) \operatorname{Im}(G_{\vec{p}}) \operatorname{Re}(\Delta G_1 G_2 \cdots G_N + G_1^* \Delta G_2 \cdots G_N + \cdots + G_1^* G_2^* \cdots \Delta G_{N-1} G_N + G_1^* G_2^* \cdots \Delta G_N).$$

(B3)

Using the identity in (A3) we obtain

$$S = (i/\gamma) \sum_{\vec{p}} (\vec{p} \cdot \vec{q}) \operatorname{Im}(G_{\vec{p}}) \operatorname{Re}(G_1^* G_2^* \cdots G_N^* - G_1 G_2 \cdots G_N) = 0.$$

(B4)

The expression in parentheses is purely imaginary and therefore $S = 0$. It is easy to see that any configuration of such starting and end points can *uniquely* be attributed to a definite class of which every diagram can be understood as an element of a cyclic permutation group, as is evident from the generation method of the class as described above. This group is again a subgroup of the full permutation group consisting of all permutations of points 1 to N. Therefore we have shown that all such diagrams containing a Γ^0 propagator vanish, irrespective of vertex corrections. As an example in Figs. 10(d)–10(n) we show one-half of a class of half-diagrams with three lines crossing Γ^0 and one additional vertex correction, the other half of the class is obtained by inverting every half diagram. Note that the two diagrams in which all points either lie on the particle or the hole line, respectively, have not been drawn because they always cancel as has been shown above.

APPENDIX C: CANCELLATION OF SUPERDIVERGING DIAGRAMS

We will here discuss how the superdiverging diagrams cancel, the general structure of which is shown in Fig. 7(a). A general proof for the cancellation of diagrams with arbitrary insertion has not been constructed, but we have investigated diagrams with up to four additional Λ^0 propagators as insertion without vertex corrections and all have been found to cancel. The mechanism is always the same; take, for example, the diagram in Fig. 7(b), which is the simplest possible superdiverging diagram with Λ^0 propagators only. Its leading contribution to $M(0, \omega)$ is

$$M^{(b)}(0, \omega) = -\sum_{\vec{p}, \vec{p}'} (\vec{p} \cdot \vec{q})^2 [\operatorname{Im}(G_{\vec{p}})]^2 |G_{\vec{p}'}|^6 \sum_{\vec{q}} [\Lambda^0(\vec{q}, \omega)]^2 = -\langle (\vec{p} \cdot \vec{q})^2 [\operatorname{Im}(G_{\vec{p}})]^2 \rangle_{\vec{p}} \langle |G_{\vec{p}}|^6 \rangle_{\vec{p}} \langle [\Lambda^0(\vec{q}, \omega)]^2 \rangle_{\vec{q}},$$

(C1)

where $\langle\ \rangle_{\vec{p}}$ implies integration over $\vec{p}$, etc. The diagrams which cancel the one in Fig. 7(b) are shown in Figs. 7(c) and 7(d); they are identical to the former one but contain one additional vertex correction over the insertion. Their contribution to M is, in similar notation

$$M^{(c)}(0,\omega) = [M^{(d)}(0,\omega)]^* = -U_0\langle(\vec{p}\cdot\hat{q})^2[\text{Im}(G_{\vec{p}})]^2\rangle_{\vec{p}}\langle|G_{\vec{p}}|^4 G_{\vec{p}}\rangle_{\vec{p}}\langle|G_{\vec{p}}|^2 G_{\vec{p}}\rangle_{\vec{p}}\langle[\Lambda^0(\vec{q},\omega)]^2\rangle_{\vec{q}}. \tag{C2}$$

To lowest order in γ/E we have $\langle|G_{\vec{p}}|^{2n}G_{\vec{p}}\rangle_{\vec{p}} = -i\gamma\langle|G_{\vec{p}}|^{2n+2}\rangle_{\vec{p}}$. Therefore the sum of all three contributions to M is

$$M^{a,b,c}(0,\omega) = -\langle(\vec{p}\cdot\hat{q})^2[\text{Im}(G_{\vec{p}})]^2\rangle_{\vec{p}}\langle|G_{\vec{p}}|^6\rangle_{\vec{p}}[1 - 2\gamma^2 U_0\langle|G_{\vec{p}}|^4\rangle_{\vec{p}}]\langle[\Lambda^0(\vec{q},\omega)]^2\rangle_{\vec{q}}. \tag{C3}$$

Now, observe that the condition for particle number conservation in (12) can also be written as $1 - U_0\langle|G_{\vec{p}}|^2\rangle_{\vec{p}} = 0$. Bearing in mind that $U_0 = \alpha\gamma$ (where α is some constant) and

$$\partial\langle|G_{\vec{p}}|^2\rangle_{\vec{p}}/\partial\gamma = -2\gamma\langle|G_{\vec{p}}|^4\rangle_{\vec{p}}$$

we obtain from this by differentiation

$$\frac{\partial U_0}{\partial\gamma}\langle|G_{\vec{p}}|^2\rangle_{\vec{p}} - 2U_0\gamma\langle|G_{\vec{p}}|^4\rangle_{\vec{p}} = 0. \tag{C4}$$

But $\partial U_0/\partial\gamma = (\gamma\langle|G_{\vec{p}}|^2\rangle_{\vec{p}})^{-1}$ and so the particle conservation relation can also be written as

$$1 - 2\gamma^2 U_0\langle|G_{\vec{p}}|^4\rangle_{\vec{p}} = 0. \tag{C5}$$

Hence the rhs of (C3) is zero and the diverging contributions have been shown to cancel. An identical mechanism of cancellation has been observed in all cases that have been investigated; it always takes a group of three diagrams with similar but not identical vertex corrections as in Figs. 7(c) and 7(d) to cancel each other.

[1]P. W. Anderson, Phys. Rev. 109, 1492 (1958).

[2]N. F. Mott, Philos. Mag. 13, 989 (1966).

[3]N. F. Mott and W. D. Twose, Adv. Phys. 10, 107 (1961); R. E. Borland, Proc. Phys. Soc. London 78, 926 (1961), Proc. R. London Ser. Soc. A 274, 529 (1963); K. Ishii, Prog. Theor. Phys. Suppl. 53, 77 (1973).

[4]F. Wegner, Z. Phys. 35, 207 (1979).

[5]E. Abrahams, P. W. Anderson, C. C. Licciardello, and T. V. Ramakrishnan, Phys. Rev. Lett. 42, 673 (1979).

[6]L. P. Gor'kov, A. I. Larkin and D. E. Khmel'nitskii, Zh. Eksp. Teor. Fiz. Pis'ma Red. 30, 248 (1979) [JETP Lett. 30, 228 (1979)].

[7]P. A. Lee, Phys. Rev. Lett. 42, 1492 (1979).

[8]W. Götze, Solid State Commun. 27, 1393 (1978); J. Phys. C 12, 1279 (1979); Philos. Mag. (in press).

[9]S. F. Edwards, Philos. Mag. 8, 1020 (1958).

[10]A. A. Abrikosov, L. P. Gor'kov, and I. E. Dzyaloshinskii, Methods of Quantum Field Theory in Statistical Physics (Prentice-Hall, Englewood Cliffs, 1969).

[11]S. V. Maleev and B. P. Toperverg, Zh. Eksp. Teor. Fiz. 69, 1440 (1975) [Sov. Phys.—JETP 42, 734 (1976)].

[12]D. Vollhardt and P. Wölfle, Phys. Rev. Lett. 45, 842 (1980).

[13]D. E. Khmel'nitskii (unpublished).

[14]P. A. Lee, J. Non-Cryst. Solids 35, 21 (1980).

[15]W. Götze, P. Prelovšek, and P. Wölfle, Solid State Commun. 30, 369 (1979).

[16]V. L. Berezinsky, Zh. Eksp. Teor. Fiz. 65, 1251 (1973) [Sov. Phys.—JETP 38, 620 (1974)].

[17]A. A. Abrikosov and I. A. Ryshkin, Adv. Phys. 27, 147 (1978).

[18]G. J. Dolan and D. D. Osheroff, Phys. Rev. Lett. 43, 725 (1979).

[19]N. Giordano, W. Gilson, and D. E. Prober, Phys. Rev. Lett. 43, 725 (1979).

[20]N. Giordano (unpublished).

[21]P. W. Anderson, E. Abrahams, and T. V. Ramakrishnan, Phys. Rev. Lett. 43, 717 (1979).